WAVE DIFFRACTION THROUGH OFFSHORE BREAKWATERS

By Robert A. Dalrymple,[1] Fellow, ASCE, and Paul A. Martin[2]

ABSTRACT: The interaction of water waves with a long linear array of offshore breakwaters is examined to determine the reflection and transmission coefficients for these structures, providing data on the sheltering afforded by these structures. Two variational methods and an eigenfunction expansion method are used to determine the reflection coefficients for waves with wavelengths longer than the distance from gap to gap in the breakwater array. The eigenfunction method is also used for breakwaters, where the spacing between the gaps is longer than the water wavelength. For this case, analogous to scattering of light by a grating, numerous monochromatic directional wave trains can be generated in the region behind (and in front of) these breakwaters, which can lead to the generation of rip currents, beach cusps, and other periodic phenomena on beaches behind the structures.

INTRODUCTION

Offshore breakwaters are used along shorelines to reduce the amount of wave energy impinging on beaches. Many are often constructed in a single straight line parallel to the coast, separated by gaps, which permit some wave action and water exchange to exist. This paper examines the propagation of the waves through these periodic gaps and determines the level of protection afforded by these breakwaters by determining reflection coefficients.

An interesting aspect of the wave field behind (and in front of) the breakwaters is that not only is the incident wave train detectable, but that when the wavelength of the incident wave train is less than the spacing of the breakwater gaps, a number of oblique wave trains may be generated as well. These oblique wave trains can lead to periodic wave-induced phenomena at the shoreline behind the breakwaters, such as nearshore circulation cells (Dalrymple 1975) and beach cusps (Dalrymple and Lanan 1976). Recently, Dalrymple et al. (1988) have shown the same phenomena occur for water waves around rows of piling.

The problem of waves impinging on a grating composed of periodically occurring line segments in the plane of the grating is classical in the areas of acoustics and optics (but not water waves). It can be solved exactly and numerous studies have been carried out, including those of Burke and Twersky (1966) and Miles (1982) in acoustics. Here the problem is solved using matched eigenfunction expansions, which lead to "dual series relations" in order to obain the correct matching conditions at the breakwater (grating). These relations are solved by a least-squares technique to find the amplitudes of the propagating and evanescent wave modes both upwave and downwave

[1]Prof. and Dir., Ctr. for Appl. Coast. Res., Dept. of Civ. Engrg., Univ. of Delaware, Newark, DE 19716.

[2]Sr. Lect., Dept. of Math., Univ. of Manchester, Manchester, M13 9PL, United Kingdom.

Note. Discussion open until April 1, 1991. To extend the closing date one month, a written request must be filed with the ASCE Manager of Journals. The manuscript for this paper was submitted for review and possible publication on March 13, 1989. This paper is part of the ***Journal of Waterway, Port, Coastal, and Ocean Engineering***, Vol. 116, No. 6, November/December, 1990. ©ASCE, ISSN 0733-950X/90/0006-0727/$1.00 + $.15 per page. Paper No. 25275.

of the breakwater. The amplitudes of the reflected and transmitted waves are calculated using this technique, and further, the wave fields in the vicinity of the breakwater are shown for several cases.

Several approximate methods can provide adequate estimates of reflection and transmission coefficients. Lamb's (1932) solution for low-frequency acoustic motion is based on a form of a matched asymptotic method, which is valid as long as the breakwaters have zero thickness (Martin and Dalrymple 1988). This method provides a simple formula; however, it is restricted to long waves. Variational methods, following Schwinger (Schwinger and Saxon 1968), can provide estimates valid for all wave lengths. These methods are compared with the exact eigenfunction expansion method.

Theoretical Analysis

The behavior of waves in the vicinity of breakwaters is modeled most simply by assuming a normally incident wave train (propagating in the positive x-direction) in water of constant depth h. The offshore breakwaters lie along the y-axis, at $x = 0$. The breakwaters are modeled as infinitely thin vertical barriers, centered at $y = \pm nb$, where $n = 1, 3, 5, \ldots, \infty$. Between the barriers are gaps of width $2l$, as shown in Fig. 1. Since the breakwaters occur periodically, the problem can be reduced to an analogous problem of a normally incident wave train propagating down a channel with imperme-

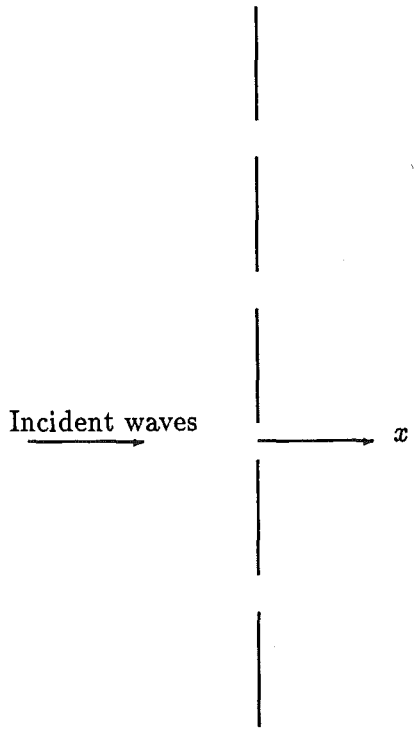

FIG. 1. Schematic Diagram of Incident Waves on Periodic Offshore Breakwater

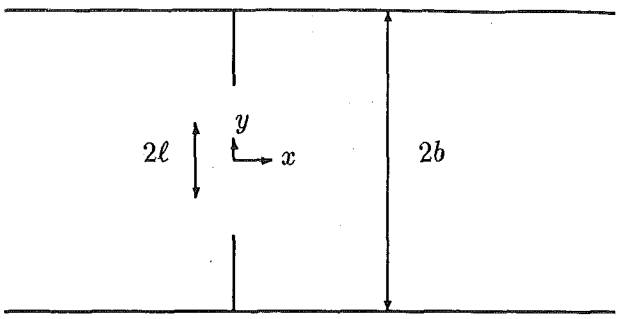

FIG. 2. Analogous Problem for Normal Incident Waves

able sidewalls into a diaphragm that occludes part of the channel at $x = 0$ (Fig. 2). The case of oblique wave incidence is discussed in Appendix I.

Our analysis will proceed under the assumptions that the fluid is incompressible and inviscid, and that the motion is irrotational. We further assume that the boundary conditions on the free surface can be linearized. The velocity potential, $\hat{\phi}(x,y,z,t)$, can be expressed as the real part of

$$\hat{\phi} = \frac{iag}{\omega}\phi(x,y)\frac{\cosh k(h+z)}{\cosh kh}e^{-i\omega t} \quad \ldots\ldots (1)$$

where a = the wave amplitude; g = the acceleration of gravity; k = the wave number; and ω = the angular frequency of the wave. The governing equation for the reduced potential, $\phi(x,y)$, is the Helmholtz equation:

$$\frac{\partial^2\phi}{\partial x^2} + \frac{\partial^2\phi}{\partial y^2} + k^2\phi = 0 \quad \ldots\ldots (2)$$

where k = the positive real solution of the dispersion relation

$$\omega^2 = gk\tanh kh \quad \ldots\ldots (3)$$

which relates the angular frequency of the wave to the water depth, h, and the wave number k. The boundary conditions that must be applied to the solutions of the Helmholtz equation are as follows: The velocities in the x-direction should be zero along the breakwaters so that there is no flow into the breakwaters; in the gap region between the breakwater, these velocities should match across the gap; and the potentials on each side should be equal in the gap to ensure that the pressure (or water surface) is continuous across the gap.

Eigenfunction Expansion Method

A solution valid on the upwave side of the breakwaters, $x < 0$, is

$$\phi_1(x,y) = e^{ikx} + \sum_{n=0}^{\infty} A_n \cos n\lambda y e^{-i\sqrt{k^2-(n\lambda)^2}x} \quad \ldots\ldots (4)$$

The first term represents the normally incident wave train, while the summation terms represent the scattered wave modes, which travel in directions

different from the incident wave direction, unless $n\lambda$ exceeds k when the waves become evanescent. The coefficient A_0 is the reflection coefficient for the reflected plane wave, traveling in the negative x-direction, which can be denoted as R. The orthogonal eigenfunctions $\{\cos n\lambda y, n = 1,2,\ldots,\infty\}$ permit a periodic solution in y and satisfy the analogous no-flow boundary conditions at $|y| = b$, provided that $\lambda = \pi/b$.

On the downwave side of the breakwaters, $x > 0$, the potential is

$$\phi_2(x,y) = e^{ikx} - \sum_{n=0}^{\infty} B_n \cos n\lambda y e^{i\sqrt{k^2-(n\lambda)^2}x} \quad \ldots\ldots (5)$$

Here the coefficients B_n give the (forward) scattered wave trains.

It is relatively easy to show that $B_n = A_n$, for all n. The velocity (in the x-direction) in the gap, $|y| \le l$, will be represented by $iF(y)$. On the upwave side, this velocity (at $x = 0$) is represented by

$$ik - \sum_{n=0}^{\infty} i\sqrt{k^2 - (n\lambda)^2}\, A_n \cos n\lambda y = \begin{cases} iF(y) & \text{for } |y| \le l \\ 0 & l < |y| \le b \end{cases} \quad \ldots\ldots (6)$$

The orthogonality of the eigenfunctions over $-b \le y \le b$ permits us to multiply each side by $\cos m\lambda y$ and to integrate over $2b$ to find equations for the A_m.

$$A_m = -\frac{1}{\sqrt{k^2 - (m\lambda)^2}\, b} \int_{-l}^{l} F(y) \cos m\lambda y dy \qquad \text{for } m > 0 \quad \ldots\ldots (7)$$

$$1 - A_0 = \frac{1}{2kb} \int_{-l}^{l} F(y) dy \quad \ldots\ldots (8)$$

The velocity (x-direction) profile across the gap can also be expanded in terms of the downwave expansion; this gives

$$B_m = -\frac{1}{\sqrt{k^2 - (m\lambda)^2}\, b} \int_{-l}^{l} F(y) \cos m\lambda y dy \qquad \text{for } m > 0 \quad \ldots\ldots (9)$$

$$1 - B_0 = \frac{1}{2kb} \int_{-l}^{l} F(y) dy \quad \ldots\ldots (10)$$

Therefore with $B_n = A_n$, the velocities in the x-direction are matched at $x = 0$ for all values of y. There are three important implications of the equality of these coefficients. First, the scattered wave field, made up of the A_n and B_n waves, is symmetric about the y-axis; there is as much upwave reflection as downwave scattering. Secondly, the x-component of the velocity at $x = 0$ is the same on both sides of the gap for the entire width of the channel as mentioned, and, finally, we have a way to relate reflection and transmission coefficients for the normally propagating wave modes. Replacing A_0 with R, the reflection coefficient for the normally incident mode, and $1 - B_0$ with T, the transmission coefficient for the transmitted wave in the normal direction, gives us the relationship between the transmission and reflection coefficients

$$T + R = 1 \quad \ldots\ldots (11)$$

Next, matching conditions are to be prescribed on the velocity and potentials at $x = 0$. The procedure to be used is not a priori obvious, as it does not follow the same methodology as used if two eigenfunction expansions (in y) were available, as in the case of the junction of two channels of different widths (Dalrymple 1989). Here, a mixed boundary condition must be prescribed. The velocities in the x-direction at $x = 0$ must be zero for $l < |y| \leq b$, the portion of the channel occluded by the breakwaters. Using the upwave potential, ϕ_1, we have the following condition:

$$ik - \sum_{n=0}^{\infty} i\sqrt{k^2 - (n\lambda)^2}\, A_n \cos n\lambda y = 0 \qquad \text{for } l < |y| \leq b \quad \ldots\ldots (12)$$

Matching the potentials across the gap, $\phi_1 = \phi_2$, for $|y| \leq l$, we have

$$\sum_{n=0}^{\infty} A_n \cos n\lambda y = 0 \qquad \text{for } |y| \leq l \quad \ldots\ldots (13)$$

The two conditions, Eqs. 12 and 13, are known as dual series relations (Sneddon 1966). They are to be solved for the values of the coefficients A_n. The conditions can be combined to make one mixed boundary condition, which specifies the potential or the velocity along the y-axis. This condition is $G(y) = 0$, for $0 \leq |y| \leq b$, where

$$G(y) = \sum_{n=0}^{\infty} A_n \cos n\lambda y \qquad \text{for } |y| \leq l \quad \ldots\ldots (14a)$$

$$G(y) = \sum_{n=0}^{\infty} \sqrt{k^2 - (n\lambda)^2}\, A_n \cos n\lambda y - k \qquad \text{for } l < |y| \leq b \quad \ldots\ldots (14b)$$

To determine the A_n, several techniques can be used, including collocation and least squares. The latter method requires that the value of $\int_{-b}^{b}|G(y)|^2 dy$ be a minimum. Minimizing this integral with respect to each of the A_n leads to the following equations:

$$\int_{-b}^{b} G^* \frac{\partial G}{\partial A_m}\, dy = 0 \qquad \text{for } m = 0, 1, 2, \ldots, \infty \quad \ldots\ldots (15)$$

where

$$\frac{\partial G}{\partial A_m} = \cos m\lambda y \qquad \text{for } |y| \leq l \quad \ldots\ldots (16a)$$

$$\frac{\partial G}{\partial A_m} = \sqrt{k^2 - (m\lambda)^2} \cos m\lambda y \qquad \text{for } l < |y| \leq b \quad \ldots\ldots (16b)$$

and G^* = the complex conjugate of G. By truncating Eq. 15 to N terms, and solving for the N values of A_n simultaneously, we obtain a complex $N \times N$ matrix equation, which we solve with the International Mathematics and Statistics Library (IMSL) routine, LEQT1C. The choice of N must be done carefully, as small values for N lead to truncation errors. Here we

typically used $N = 75$, although in most cases far fewer evanescent modes are needed.

VARIATIONAL APPROACH

An alternative approach to determine the reflection coefficient for this problem is the variational approach of Schwinger (Schwinger and Saxon 1968). The method is considered only for the case of plane waves in the upwave region ($x < 0$). The advantage of the variational approach is the far-simpler estimate of the reflection coefficient.

The matching of the potential, Eq. 13, can be rewritten in terms of the reflection coefficient associated with the plane wave.

$$R + \sum_{n=1}^{\infty} A_n \cos n\lambda y = 0 \qquad \text{for } |y| \leq l \ldots\ldots\ldots\ldots\ldots\ldots\ldots\ldots \quad (17)$$

However, Eq. 17 can be rewritten using the values of the coefficients (A_n) from the matching condition for the velocities, Eq. 8; namely

$$R - \sum_{n=1}^{\infty} \int_{-l}^{l} \frac{F(\zeta) \cos n\lambda d\zeta}{\sqrt{k^2 - (n\lambda)^2 b}} \cos n\lambda y = 0 \qquad \text{for } |y| \leq l \ldots\ldots\ldots\ldots\ldots\ldots \quad (18)$$

Further, the first term can be expressed as

$$R = R \frac{\int_{-l}^{l} F(\zeta) d\zeta}{2bk(1 - R)} \ldots\ldots\ldots\ldots\ldots\ldots\ldots\ldots\ldots\ldots\ldots\ldots\ldots\ldots\ldots\ldots \quad (19)$$

since the fraction term has a value of unity, from Eq. 8. Next, multiply both sides of the matching condition by the velocity profile, $iF(y)$, and integrate over $|y| \leq l$ to remove the y dependency in Eq. 18. This yields

$$\frac{R}{1 - R} = \frac{\sum_{n=1}^{\infty} \frac{2k}{\sqrt{k^2 - (n\lambda)^2}} \left[\int_{-l}^{l} F(\zeta) \cos n\lambda\zeta d\zeta \right]^2}{\left[\int_{-l}^{l} F(\zeta) d\zeta \right]^2} \ldots\ldots\ldots\ldots\ldots\ldots\ldots\ldots \quad (20)$$

This final form for R is the variational expression, which can be shown to be second-order accurate if the assumed velocity profile is first-order accurate. Further, it is independent of the magnitude of the assumed velocity, which cancels out.

The simplest assumption for $F(y)$ is that the velocity is constant across the gap. This results in the following form for the ratio:

$$\frac{R}{1 - R} = \sum_{n=1}^{\infty} \frac{2k}{\sqrt{k^2 - (n\lambda)^2}} \left(\frac{\sin n\lambda l}{n\lambda l} \right)^2 \ldots\ldots\ldots\ldots\ldots\ldots\ldots\ldots\ldots\ldots\ldots\ldots \quad (21)$$

This series converges quite rapidly (the terms decay like n^{-3}); 20–30 terms provide sufficient accuracy, but note that complex arithmetic is needed due to the form of the denominator.

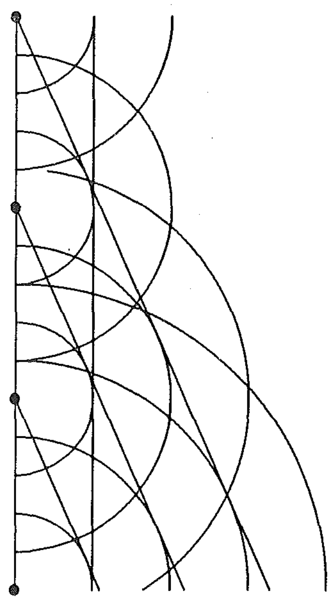

FIG. 3. Huygen's Principle Explanation for Generation of Several Wave Trains from Periodic Breakwater Gaps. By Superimposing Wave Crests from Various Sources, Straight Lines Show Some of Resulting Wave Trains

A better representation of the velocity profile across the gap, $F(y)$, is

$$F(y) = \frac{Ul}{\sqrt{l^2 - y^2}} \qquad (22)$$

where U = a constant (Sommerfeld 1964). The denominator in this form ensures that singularities in the velocity occur at the ends of the breakwaters, as predicted by potential flow around a barrier. Substituting this form of $F(y)$ into Eq. 20, gives

$$\frac{R}{1 - R} = \sum_{n=1}^{\infty} \frac{2k}{\sqrt{k^2 - (n\lambda)^2}} J_0^2(n\lambda l) \qquad (23)$$

where J_0 = a Bessel function. As shown later, this last representation is the better of the two. However, it converges more slowly (the terms decay like n^{-2}), requiring about four times as many terms for the same accuracy.

Both of the variational solutions are functions of two parameters, namely, kb, which is the ratio of the breakwater spacing to the wavelength, and l/b, the gap width to breakwater spacing ratio. Further, explicit resonances occur ($|R| = 1$) whenever $kb = n\pi$, corresponding to $k = n\lambda$. These cases correspond to cross-tank seiching, or sloshing, as an integer number of wave lengths fit exactly across the width, $2b$.

For long waves, $kb << \pi$, Lamb's (1932) method gives another explicit expression (rewritten in our notation):

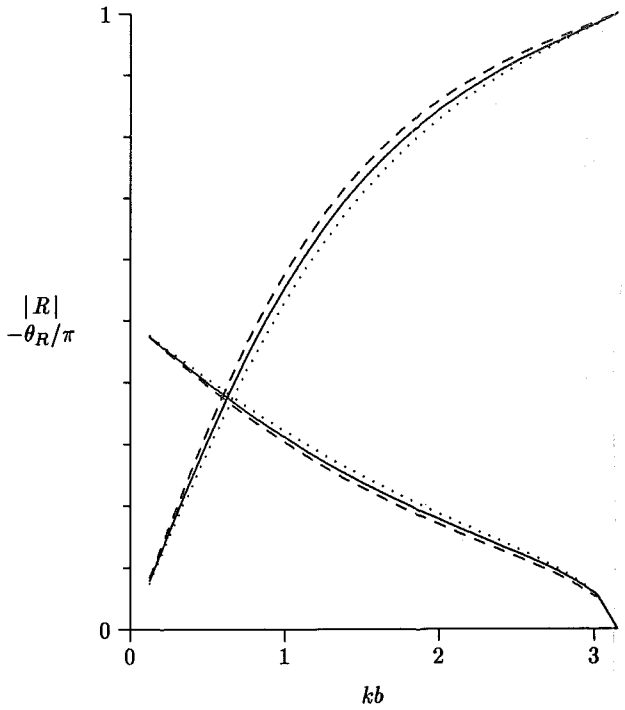

FIG. 4. Amplitude (Lower Curves at $kb = 0$) and Phase of Reflection Coefficient for $l/b = 0.25$, as Computed by Eigenfunction Method and Two Variational Methods. Eigenfunction Method: ———; Constant Velocity Variational Method: – – –; and Sommerfeld's Velocity Approximation: ·····

$$\frac{R}{1-R} = \frac{2i}{\pi} kb \log\left[\sin\left(\frac{\lambda l}{2}\right)\right] \quad \text{(24)}$$

COMMENTS

The wave fields, upwave and downwave of the breakwaters, consist of the incident plane wave train, propagating in the x-direction, plus, when $kb > \pi$, the progressive scattered waves, which consist of pairs of intersecting waves, traveling at angles, $\pm\tan^{-1}(n\lambda/\sqrt{k^2 - (n\lambda)^2})$ to the x-axis. There is only a finite number of these oblique wave trains, as their propagation angles must be between $-\pi/2$ and $+\pi/2$. Finally, there are the evanescent modes, with the y-component of the wave number, $n\lambda > k$. These wave modes serve to provide matching at the breakwater gaps, but then decay exponentially away from the breakwater.

The number of progressive oblique wave trains is determined by the requirement that

$$\sqrt{k^2 - (n\lambda)^2} \geq 0 \quad \text{(25)}$$

Solving as an equality, we have

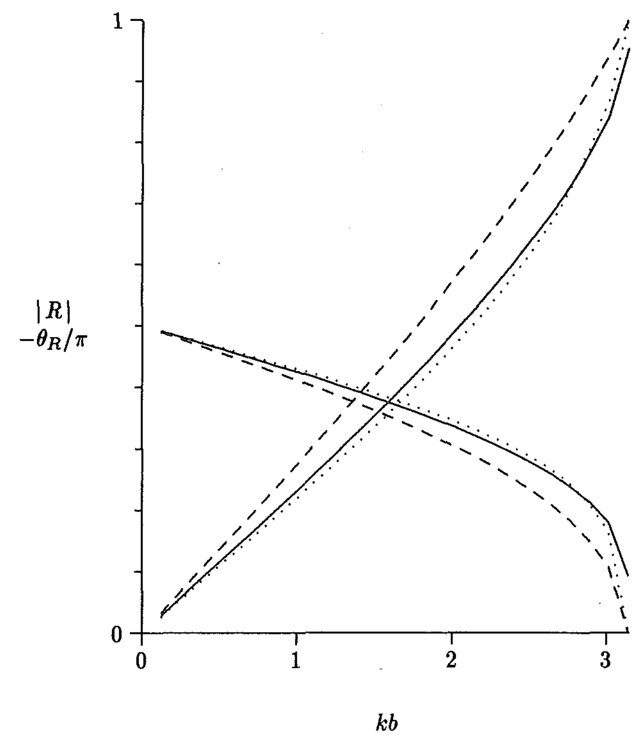

FIG. 5. Amplitude (Lower Curves at $kb = 0$) and Phase of Reflection Coefficient for $l/b = 0.50$, as Computed by Eigenfunction Method and Two Variational Methods. Curves Are Defined in Fig. 4

$$n = \frac{k}{\lambda} = \frac{2b}{L} = \frac{kb}{\pi} \quad (26)$$

where L = the wavelength of the incident wave field. Thus, when $kb < \pi$, oblique wave trains are not generated; only the wave trains propagating in the x-direction exist.

The presence of the oblique wave trains, predicted by the eigenfunction analysis, is explained easily using Huygens' principle, as illustrated in Fig. 3 (French 1971). If each breakwater gap is viewed as a diffraction source, producing circular waves, then, by superposition of the diffracted waves from all the gaps, the wave trains and their directions can be determined. For example, if a straight line is drawn connecting all the circular wave patterns that passed through the gaps at the same instant, the normally transmitted wave train results (as shown by the vertical lines in Fig. 3). However, if the wave issuing from one gap is connected to the wave crest that passed through the neighboring gap one wave period before, and to the wave crest of the next gap from two wave periods before and so on, a wave train is created by superposition, traveling in a different direction. There is also the companion wave train traveling at exactly the opposite angle to the x-axis.

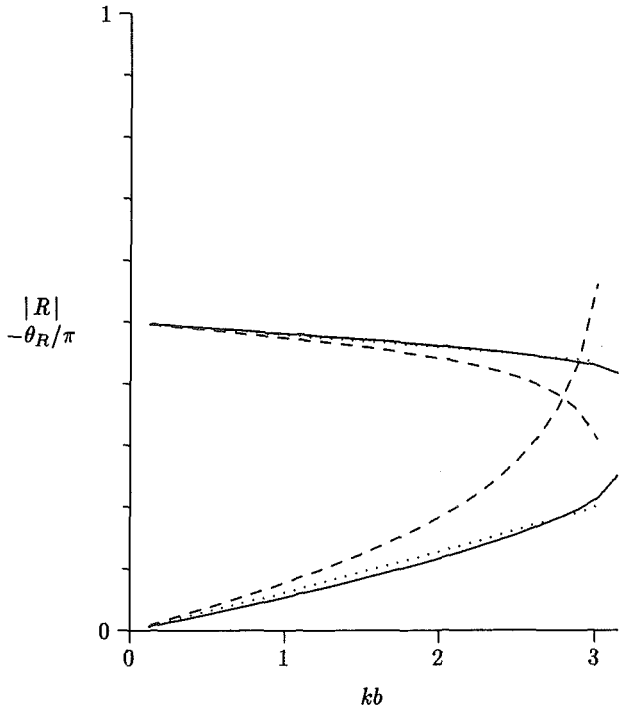

FIG. 6. Amplitude (Lower Curves at $kb = 0$) and Phase of Reflection Coefficient for $l/b = 0.75$, as Computed by Eigenfunction Method and Two Variational Methods. Curves Are Defined in Fig. 4

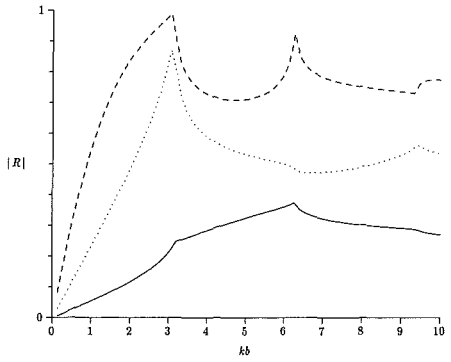

FIG. 7. Amplitude of Reflection Coefficients from Eigenfunction Method for Different Dimensionless Gap Widths. $l/b = 0.25$ – – – –; $l/b = 0.50$: ·····; and $l/b = 0.75$: ————

COMPARISON OF METHODS

First, we examine the range $0 < kb < \pi$, such that only the normally incident waves are progressive; that is, there are no other directional wave trains present. In this situation, the variational methods and the eigenfunction methods can be compared. In Figs. 4, 5, and 6, the amplitude and phase of the reflection coefficients are shown for the three methods as a function of the dimensionless channel width, kb, for different dimensionless gap widths, $l/b = 0.25$, 0.50, and 0.75. The amplitude and phase are defined by

$$R = |R|e^{i\theta_R}$$

For the smallest value of l/b, the variational approaches, which are far easier

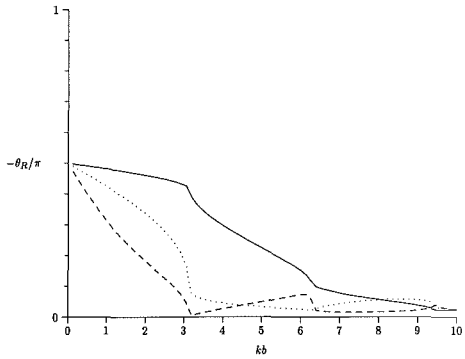

FIG. 8. Phase of Reflection Coefficients from Eigenfunction Method for Different Dimensionless Gap Widths, l/b. Curves Are Defined in Fig. 7

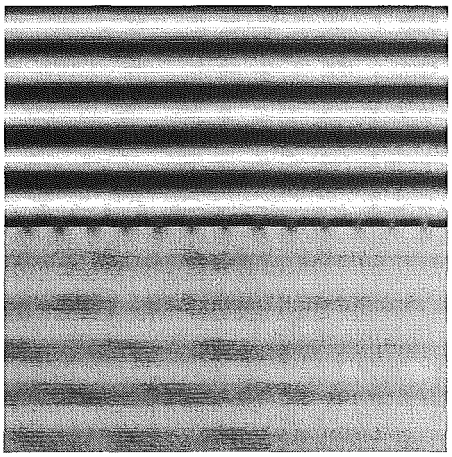

FIG. 9. Instantaneous Water-Surface Displacement in Front of and behind Offshore Breakwater Array. Five Wave Lengths Are Shown on Each Side, $kb = 2.35$ and $l/b = 1/9$, and Incident Wave Train Comes from Top of Figure

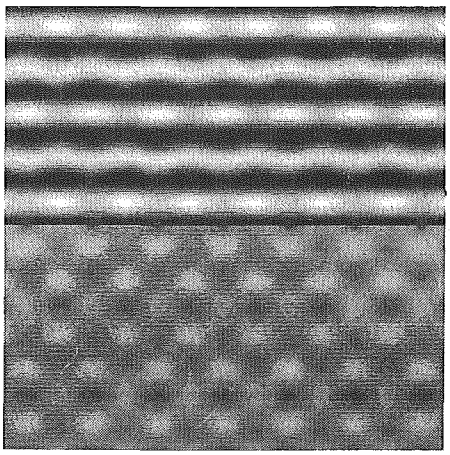

FIG. 10. Instantaneous Water-Surface Displacement in Front of and behind Offshore Breakwater Array. $kb = 4.7$ and $l/b = 1/9$

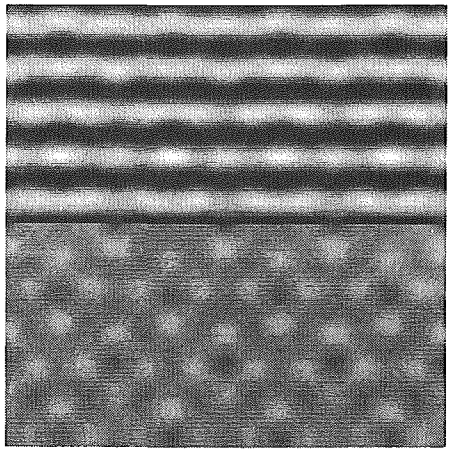

FIG. 11. Instantaneous Water-Surface Displacement in Front of and behind Offshore Breakwater Array. $kb = 9.7$ and $l/b = 1/9$

to compute than the eigenfunction method, bracket the eigenfunction method results. (Note that 75 terms in the series were taken for all three methods.) However, as the gap spacing increases, the variational method based on the Sommerfeld velocity condition proves to be far better than that using the constant velocity profile in the gap.

Lamb's method, Eq. 24, although not shown in the figures, compares extremely well with the eigenfunction solution for small kb and small l/b. As kb increases (greater than unity), Lamb's solution for $|R|$ increasingly underestimates the correct answer.

In Figs. 7 and 8, the amplitude and phase are again plotted for the nor-

mally incident mode as kb varies from 0 to 10. Note that at $kb = n\pi$, $n = 1, 2, 3, \ldots$, there is an increase in the reflection coefficient as the cross-tank modes are excited.

In Figs. 9–11, the instantaneous water-surface elevations are shown for various kb values over an area equal to 10 (incident) wavelengths in each direction to illustrate the directional nature of the waves scattered by the breakwaters. The breakwater array is located on a horizontal line passing through the center of the figure, and the incident wave train arrives from the top of the figure. The water-surface elevations are shaded in these figures with the highest water levels being white. For each case, the dimensionless gap width, l/b, is kept constant as $1/9$, and kb is varied. For Fig. 9, kb is less than π, so only a long wave is transmitted. For Fig. 10, $\pi < kb < 2\pi$, and there are three wave trains on the downwave side of the breakwater. This figure compares qualitatively with the ripple tank experiment illustrated by French (1971). Finally, for Fig. 11, $2\pi < kb < 3\pi$, five wave trains are present.

Conclusions

The reflection and transmission of waves incident on a segmented breakwater are readily computed by several means. When the wavelength is long compared to the gap spacing, several methods (eigenfunction and variational) are available to compute the reflection coefficients accurately. Of the variational methods, the assumption of a realistic velocity profile in the gap between the breakwaters yields a better comparison to the eigenfunction approach.

For smaller wavelengths, the eigenfunction expansion method is used to compute the reflection coefficients for the breakwater gap, as the variational methods used here are no longer valid when $kb > \pi$. For this short wave case, other wave trains exist, which travel in directions other than the normal direction. These waves can, in fact, lead to interesting coastal processes behind the breakwaters.

Realistic fluid effects, such as the influence of viscosity and flow separation in the vicinity of the heads of the breakwaters, have been neglected. These will play a role in reducing the transmitted wave height.

Acknowledgment

This work was supported in part by NOAA Office of Sea Grant, U.S. Department of Commerce, under Grant No. NA86AA-D-SG-040 (R/OE-1). The U.S. government is authorized to produce and distribute reprints for governmental purposes, notwithstanding any copyright notation that may appear herein.

Appendix I. Theoretical Approach for Oblique Incidence

The potential in the upwave region, including the obliquely incident wave train, can be expressed as

$$\phi_1 = e^{i\sqrt{k^2-\lambda_0^2}x}e^{i\lambda_0 y} + \sum_{n=-\infty}^{\infty} A_n e^{-i\sqrt{k^2-(n\lambda)^2}x}e^{in\lambda y} \quad \ldots\ldots\ldots\ldots\ldots\ldots\ldots\ldots\ldots\ldots \quad (27)$$

where λ_0 = the wavenumber in the y-direction for the incident wave train. The direction of the wave train is found from the relationship, $\lambda_0 = k \sin(\theta_0)$, where θ_0 is the direction of the wave train to the x-axis.

We can expand the first term in terms of $e^{in\lambda y}$ by

$$e^{i\lambda_0 y} = \sum_{n=-\infty}^{\infty} C_n e^{in\lambda y}$$

where we find, by orthogonality, that

$$C_n = \frac{\sin(\lambda_0 - n\lambda)b}{(\lambda_0 - n\lambda)b} \quad \ldots\ldots\ldots\ldots\ldots\ldots\ldots\ldots\ldots\ldots\ldots\ldots\ldots\ldots\ldots\ldots \quad (28)$$

Rewriting ϕ_1, we have

$$\phi_1 = \sum_{n=-\infty}^{\infty} \frac{\sin(\lambda_0 - n\lambda)b}{(\lambda_0 - n\lambda)b} e^{i\sqrt{k^2-\lambda_0^2}x} e^{in\lambda y} + \sum_{n=-\infty}^{\infty} A_n e^{-i\sqrt{k^2-(n\lambda)^2}x} e^{in\lambda y} \quad \ldots\ldots\ldots\ldots \quad (29)$$

The potential in the downwave region is assumed to be

$$\phi_2 = \sum_{n=-\infty}^{\infty} \frac{\sin(\lambda_0 - n\lambda)b}{(\lambda_0 - n\lambda)b} e^{i\sqrt{k^2-\lambda_0^2}x} e^{in\lambda y} - \sum_{n=-\infty}^{\infty} A_n e^{i\sqrt{k^2-(n\lambda)^2}x} e^{in\lambda y} \quad \ldots\ldots\ldots\ldots \quad (30)$$

which guarantees that the velocity through the gap matches on both sides.

Now, using the same matching conditions as before, we obtain the condition, $G(y) = 0$, where

$$G(y) = \begin{cases} \sum_{n=0}^{\infty} A_n e^{in\lambda y} & \text{for } |y| \le l \\ \sum_{n=0}^{\infty} [C_n \sqrt{k^2 - \lambda_0^2} - A_n \sqrt{k^2 - (n\lambda)^2}] e^{in\lambda y} & \text{for } l < |y| \le b \end{cases} \quad \ldots\ldots \quad (31)$$

where the C_n's are defined. Minimizing as before, a complex matrix equation results for the A_n's.

APPENDIX II. REFERENCES

Burke, J. E., and Twersky, V. (1966). "On scattering of waves by the infinite grating of elliptic cylinders." *IEEE Trans. Antennas and Propagation,* Institute of Electrical and Electronics Engineering, 14, 465–480.

Dalrymple, R. A. (1975). "A mechanism for rip currents generation on an open coast." *J. Geophys. Res.,* 80(24), 3485–3487.

Dalrymple, R. A. (1989). "Water waves past abrupt channel transitions." *Appl. Ocean Res.,* 11(4), 170–175.

Dalrymple, R. A., and Lanan, G. A. (1976). "Beach cusps formed by intersecting waves." *Geological Soc. of America Bulletin,* 87(1), 57–60.

Dalrymple, R. A., Seo, S. N., and Martin, P. A. (1988). "Water wave scattering by rows of circular cylinders." *Proc. 21st Int. Coastal Engrg. Conf.,* ASCE, 2216–2228.

French, A. P. (1971). *Vibrations and waves.* W. W. Norton & Co., New York, N.Y.

Lamb, H. (1932). Hydrodynamics. Cambridge Univ. Press, Cambridge, England.

Martin, P. A., and Dalrymple, R. A. (1988). "Scattering of long waves by cylin-

drical obstacles and gratings using matched asymptotic expansions." *J. Fluid Mech.*, 188, 465–490.
Miles, J. W. (1982). "On Rayleigh scattering by a grating." *Wave Motion,* 4, 285–292.
Schwinger, J., and Saxon, D. S. (1968). *Discontinuities in waveguides: Notes on lectures by Julian Schwinger*. Gordon and Breach Sci. Pub., New York, N.Y.
Sneddon, I. N. (1966). *Mixed boundary value problems in potential theory*. North Holland Publishing Co., Amsterdam, The Netherlands.
Sommerfeld, A. (1964). "Optics." *Lectures on theoretical physics,* IV, Academic Press, New York, N.Y.